Conjugate natural convection in three-dimensional differentially heated cubic partitioned cavity filled with air and water

Conference Paper *in* AIP Conference Proceedings · January 2021

DOI: 10.1063/5.0037525

CITATIONS
9

READS
253

4 authors:

Mukit Amin
Bangladesh University of Engineering and Technology
1 PUBLICATION **9** CITATIONS
SEE PROFILE

Faisal Tushar
Clemson University
3 PUBLICATIONS **12** CITATIONS
SEE PROFILE

Delower Hossen
Bangladesh University of Engineering and Technology
1 PUBLICATION **9** CITATIONS
SEE PROFILE

Sumon Saha
Bangladesh University of Engineering and Technology
232 PUBLICATIONS **1,820** CITATIONS
SEE PROFILE

Conjugate natural convection in three-dimensional differentially heated cubic partitioned cavity filled with air and water

Cite as: AIP Conference Proceedings **2324**, 050026 (2021); https://doi.org/10.1063/5.0037525
Published Online: 25 February 2021

Mukit Amin, Faisal Alam Tushar, Delower Hossen, and Sumon Saha

Conjugate Natural Convection in Three-Dimensional Differentially Heated Cubic Partitioned Cavity Filled with Air and Water

Mukit Amin[a)], Faisal Alam Tushar[b)], Delower Hossen[c)] and Sumon Saha[d)]

Department of Mechanical Engineering, Bangladesh University of Engineering and Technology, Dhaka-1000, Bangladesh

[d)]Corresponding author: sumonsaha@me.buet.ac.bd
[a)]aminmukit@gmail.com
[b)]faisalalamtushar@gmail.com
[c)]dnrdelower@gmail.com

Abstract. Conjugate natural convection heat transfer in a three-dimensional differentially heated, partitioned cubic cavity filled with air in one side and water in other side is investigated numerically in this study. Fluid flow and heat transfer characteristics are governed by continuity, momentum and energy equations, which are solved using Galerkin finite element method. Effect of different positions of the solid vertical partition inside the cavity on the overall heat transfer and fluid flow scenario is observed here. Simulation is performed within a range of Rayleigh number based on the properties of air ($10^3 \leq Ra_a \leq 10^5$). Results are obtained in the form of isosurface plots of velocity and temperature and contour plots of heat function within the computational domain. Besides, average Nusselt numbers of both hot and cold walls are evaluated and compared with a two-dimensional model for different positions of the solid partition. From the comparative analysis, it is found that partition position has strong influence on overall heat transfer rate.

INTRODUCTION

Natural convection is characterized by density difference that occurs when fluid is heated. Motion of the fluid is solely caused by the difference in density resulting from temperature gradient across the fluid layers and is not externally aided by a pump or fan. When both conduction and natural convection heat transfer simultaneously occur in a system consists of solid and fluid domains, the mechanism is called conjugate natural convection heat transfer. There is a huge interest in the field of engineering for conjugate natural convection heat transfer, e.g., cooling of molten metals, passive cooling of electronic device, solar energy collector, passive heat exchangers, etc.

Anderson and Bejan [1], at first, studied conjugate natural convection heat transfer in a partitioned differentially heated cavity filled with water. Based on the Oseen linearization method, they solved the problem both theoretically and experimentally and evaluated the overall heat transfer rate with varying number of vertical partitions. The effect of wall conduction and radiation on natural convection in a square cavity was analyzed by Kim and Viskanta [2]. Kaminski and Prakash [3] then investigated conjugate natural convection inside a two-dimensional square enclosure by assuming the enclosure to be bounded by one thick wall and three thin walls. Nishimura *et al.* [4] studied influence of thin conducting partition on natural convection inside a rectangular cavity filled with water and also introduced multiple partitions inside the computational domain. Furthermore, similar studies had been done by Kangni *et al.* [5] considering air as the working fluid inside the cavity. They also varied thermal conductivity ratio of the partition material and the working fluid and found that the heat transfer rate decreased with increasing partition number at high Rayleigh number for all conductivity ratio. The effect of the aspect ratio on natural convection inside rectangular cavities having partition walls was observed by Ghosh *et al.* [6]. Besides, Saha *et al.* [7] investigated the effect of coupled thermal boundary layer induced by a thin wavy conducting partition inside a square cavity. They

Proceedings of the 13th International Conference on Mechanical Engineering (ICME2019)
AIP Conf. Proc. 2324, 050026-1–050026-8; https://doi.org/10.1063/5.0037525
Published by AIP Publishing. 978-0-7354-4068-5/$30.00

found that increase of amplitude of the partition wall reduced the heat transfer inside the cavity. Recently, Khatamifar *et al.* [8] investigated the effect of Rayleigh number, partition thickness and partition position on conjugate natural convection inside a partitioned cavity. Their work was done for high Rayleigh number (10^5–10^9). Apart from considering only single working fluid, Öztop *et al.* [9] investigated conjugate natural convection heat transfer in a vertically divided enclosure by a solid partition filled with two different fluids, air and water. Results were obtained in terms of Grashof number, partition thickness and partition position. Recently, Kushwaha *et al.* [10] extended the works of Öztop *et al.* [9] considering the influence of Rayleigh number as well as thickness, position and thermal conductivity of the solid partition on the thermal performance inside the partitioned cavity separated by air-water zones. Compared with its 2D counterpart, the 3D enclosure is a more realistic configuration that is frequently encountered in engineering applications. The convective flow is mainly three-dimensional, since its patterns are more complex and involves more influential factors to characterize the system. Conjugate mixed convection inside a three-dimensional cubic enclosure separated by the solid partition and having a inner rotating adiabatic circular cylinder was examined by Selimefendigil and Öztop [11]. Their investigation implied that heat transfer increased for higher Richardson number as well as angular speed of the cylinder.

The concept of heatline was first introduced by Kimura and Bejan [12] for visualizing convection and thermal energy flow. Later, Hooman and Gurgenci [13] visualized heatline of natural convection in a porous cavity occupied by a fluid with temperature-dependent viscosity. Recently, Hussein and Hussain [14] performed heatline visualization of natural convection heat transfer in an inclined wavy cavity filled with nanofluids and subjected to a discrete isoflux heating.

From the above literature survey, it is found that no work has been done considering a cubic partitioned cavity filled with two different fluids in two separate regions. Hence, the present study focuses to investigate conjugate natural convection heat transfer in a differentially heated partitioned cubic cavity filled with air and water. Results are presented in the form of isosurface plots of fluid velocity and temperature as well as visualization of heatline in 3D system. Attention is given to examine and compare both 2D [10] and 3D analysis of thermal performance of the cavity with the variation of partition position.

PHYSICAL MODELING

A 3D cubic cavity of length L, vertically partitioned by a heat conducting solid wall of thickness $e = 0.1L$ is shown in Fig. 1. The left and the right walls are maintained at constant temperatures T_C and T_H ($T_H > T_C$) respectively, while the other walls are assumed to be adiabatic. The solid partition is vertically placed at a distance c from the left wall, which separates the entire cavity into two convection regions and one conduction region. The partition material is selected as brick with thermal conductivity k_s = 20.68 W/mK [15]. Left and right convective regions are filled with air and water respectively. Hence, the air domain is in contact with the cold wall and the water domain is in contact with the hot wall. The effect of gravity is acting vertically in negative z-direction. The thermo-physical properties of air and water considered in the present study are listed in Table 1.

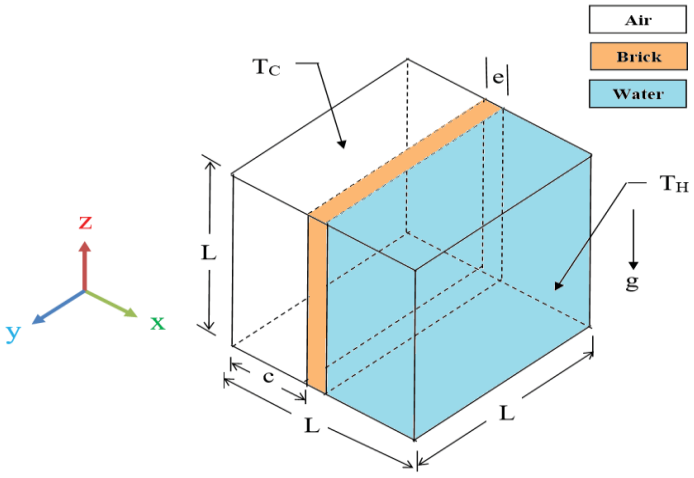

FIGURE 1. Schematic diagram of 3D model of a partitioned cubic cavity filled with air (left domain) and water (right domain) in Cartesian coordinate system.

TABLE 1. Thermo-physical properties of working fluids taken at 20ºC [15].

Property	Symbol	Unit	Air	Water
Density	ρ	kg/m^3	1.204	998.0
Specific Heat	C_p	J/kgK	1007	4182
Thermal Conductivity	k	W/mK	0.02514	0.598
Dynamic Viscosity	μ	Ns/m^2	1.825×10^{-5}	0.195×10^{-3}
Thermal diffusivity	α	m^2/s	2.074×10^{-5}	6.98×10^{-6}
Prandtl Number	Pr	–	0.7309	7.01

MATHEMATICAL MODELING

Both air and water are considered as Newtonian fluid. Flow inside the cavity is considered to be three-dimensional, laminar, steady state and incompressible. The governing continuity, momentum, and energy equations in non-dimensional form applicable for the present model are written as follows:

Air Domain:

$$\frac{\partial U}{\partial X}+\frac{\partial V}{\partial Y}+\frac{\partial W}{\partial Z}=0, \tag{1}$$

$$U\frac{\partial U}{\partial X}+V\frac{\partial U}{\partial Y}+W\frac{\partial U}{\partial Z}=-\frac{\partial P}{\partial X}+Pr_a\left(\frac{\partial^2 U}{\partial X^2}+\frac{\partial^2 U}{\partial Y^2}+\frac{\partial^2 U}{\partial Z^2}\right), \tag{2}$$

$$U\frac{\partial V}{\partial X}+V\frac{\partial V}{\partial Y}+W\frac{\partial V}{\partial Z}=-\frac{\partial P}{\partial Y}+Pr_a\left(\frac{\partial^2 V}{\partial X^2}+\frac{\partial^2 V}{\partial Y^2}+\frac{\partial^2 V}{\partial Z^2}\right), \tag{3}$$

$$U\frac{\partial W}{\partial X}+V\frac{\partial W}{\partial Y}+W\frac{\partial W}{\partial Z}=-\frac{\partial P}{\partial Z}+Pr_a\left(\frac{\partial^2 W}{\partial X^2}+\frac{\partial^2 W}{\partial Y^2}+\frac{\partial^2 W}{\partial Z^2}\right)+Ra_aPr_a\theta, \tag{4}$$

$$U\frac{\partial \theta}{\partial X}+V\frac{\partial \theta}{\partial Y}+W\frac{\partial \theta}{\partial Z}=\frac{\partial^2 \theta}{\partial X^2}+\frac{\partial^2 \theta}{\partial Y^2}+\frac{\partial^2 \theta}{\partial Z^2}, \tag{5}$$

Water Domain:

$$\frac{\partial U}{\partial X}+\frac{\partial V}{\partial Y}+\frac{\partial W}{\partial Z}=0, \tag{6}$$

$$\frac{\rho_w}{\rho_a}\left(U\frac{\partial U}{\partial X}+V\frac{\partial U}{\partial Y}+W\frac{\partial U}{\partial Z}\right)=-\frac{\partial P}{\partial X}+\frac{\mu_w}{\mu_a}Pr_a\left(\frac{\partial^2 U}{\partial X^2}+\frac{\partial^2 U}{\partial Y^2}+\frac{\partial^2 U}{\partial Z^2}\right), \tag{7}$$

$$\frac{\rho_w}{\rho_a}\left(U\frac{\partial V}{\partial X}+V\frac{\partial V}{\partial Y}+W\frac{\partial V}{\partial Z}\right)=-\frac{\partial P}{\partial Y}+\frac{\mu_w}{\mu_a}Pr_a\left(\frac{\partial^2 V}{\partial X^2}+\frac{\partial^2 V}{\partial Y^2}+\frac{\partial^2 V}{\partial Z^2}\right), \tag{8}$$

$$\frac{\rho_w}{\rho_a}\left(U\frac{\partial W}{\partial X}+V\frac{\partial W}{\partial Y}+W\frac{\partial W}{\partial Z}\right)=-\frac{\partial P}{\partial Z}+\frac{\mu_w}{\mu_a}Pr_a\left(\frac{\partial^2 W}{\partial X^2}+\frac{\partial^2 W}{\partial Y^2}+\frac{\partial^2 W}{\partial Z^2}\right)+\frac{\rho_w}{\rho_a}Ra_aPr_a\theta, \tag{9}$$

$$U\frac{\partial \theta}{\partial X}+V\frac{\partial \theta}{\partial Y}+W\frac{\partial \theta}{\partial Z}=\frac{\alpha_w}{\alpha_a}\left(\frac{\partial^2 \theta}{\partial X^2}+\frac{\partial^2 \theta}{\partial Y^2}+\frac{\partial^2 \theta}{\partial Z^2}\right), \tag{10}$$

where, X, Y, Z are the non-dimensional Cartesian coordinates, U, V *and* W are the non-dimensional velocity components in the X, Y and Z directions respectively, P is the non-dimensional pressure, θ is the non-dimensional temperature, α, μ and ρ are thermal diffusivity, dynamic viscosity and mass density of the working fluid respectively, Ra and Pr are Rayleigh and Prandtl numbers respectively. The conduction heat transfer through the partition wall is governed by the following energy equation:

$$k_r\left(\frac{\partial^2 \theta}{\partial X^2}+\frac{\partial^2 \theta}{\partial Y^2}+\frac{\partial^2 \theta}{\partial Z^2}\right)=0, \tag{11}$$

where, $k_r = k_s/k_a$ is the ratio of thermal conductivity of the solid partition and air. The subscripts 'a', 'w' and 's' represent property for air, water and solid partition respectively. The boundary conditions considered for this problem is presented in non-dimensional form in Table 2.

TABLE 2. Non-dimensional boundary conditions considered for the computational domain.

Boundary	Thermal Condition	Velocity Condition
Left wall	$\theta = 0$	
Right wall	$\theta = 1$	
Top, bottom, front and rear walls	$\partial\theta/\partial N = 0$	$U = V = W = 0$ (for all walls)
Partition wall (left)	$k_r(\partial\theta/\partial X)_{solid} = (\partial\theta/\partial X)_{air}$	
Partition wall (right)	$(k_s/k_w)(\partial\theta/\partial X)_{solid} = (\partial\theta/\partial X)_{water}$	

Here, N is the non-dimensional wall normal distance. The average Nusselt number along hot wall can be expressed as:

$$Nu = \int_0^1 \int_0^1 \left.\frac{\partial\theta}{\partial X}\right|_{X=0} dYdZ\,. \tag{12}$$

In order to visualize the heatline contours, the non-dimensional heat function Π_Y on the X-Z plane is evaluated using the following relation:

$$\frac{\partial^2\Pi_Y}{\partial X^2} + \frac{\partial^2\Pi_Y}{\partial Z^2} = \frac{\partial(U\theta)}{\partial Z} - \frac{\partial(W\theta)}{\partial X}\,. \tag{13}$$

NUMERICAL SIMULATION AND MODEL VALIDATION

The governing equations (1) – (11) along with boundary conditions as listed in Table 2 are solved numerically using Galerkin finite element method. The 3D computation domain is at first discretized using non-uniform tetrahedral elements with finer mesh elements near the solid walls. The optimum element number is selected as 67767 after performing a thorough mesh independent test. The present model is validated by regenerating the works of Kimura and Bejan [12] and Khatamifar *et al.* [8] (see Fig. 2). At first, qualitative comparison of heatline contour plots between Kimura and Bejan [12] and the present simulation is shown in Fig. 2(a) and (b) respectively. It is observed that the comparison reveals quite good agreement of both results. Next, a quantitative verification in terms of average Nusselt number obtained by the present model and Khatamifar *et al.* [8] is carried out as shown in Fig. 2(c). Both plots of *Nu* display an excellent matching of these works. Hence, it can be concluded that the present model can be further used to predict the flow and thermal characteristics in a partitioned cubic cavity within reasonable accuracy.

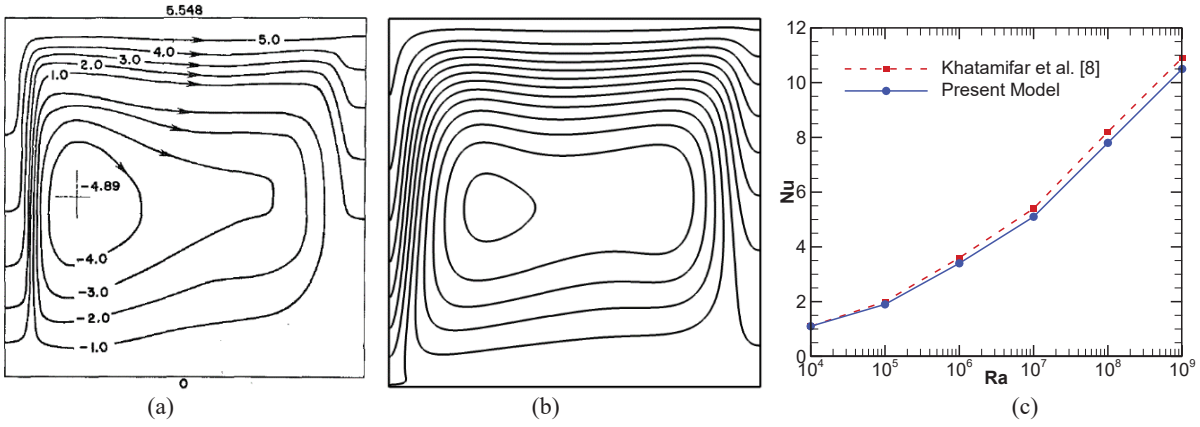

FIGURE 2. Verification of heatline contour plot obtained from (a) Kimura and Bejan [12] with that of (b) the present model and (c) validation of average Nusselt number evaluated from the present model with that of Khatamifar *et al.* [8].

RESULTS AND DISCUSSION

The parametric simulations are performed for three different partition positions, $C = c/L = 0.25$, 0.50 and 0.75 within the range of Rayleigh number ($10^3 \le Ra_a \le 10^5$). At first, the visualization of flow and thermal fields is

presented in terms of isosurface contour maps of velocity, isosurface plots of temperatures, 3D heatline plots. Next, a comparison of average Nusselt number of both hot and cold walls for different partition positions are shown.

Visualization of Flow and Thermal Fields

Figure 3 displays the visualization of flow field inside the partitioned cavity in terms of isosurface contour maps of velocity. From the figure, it is found that for smaller domain size, the contour maps of velocity field are very compact and at larger domain size, those maps tend to become more dispersed and stretch out with increasing Ra_a. Stability and strength of fluid flow depend on the type of the working fluid used in each convective domain. At lower Rayleigh number, flow circulation inside the separate domain takes the form of uniform shape representing lower heat transfer. Moreover, the level of magnitude of velocity inside the air domain is always higher than that of the water domain. Hence, the circulation strength becomes higher at the air filled domain representing higher heat transfer rate.

Now the visualization of thermal fields is presented in terms of isosurface plots of temperature and 3D heatline plots as shown in Figs. 4 and 5 respectively. From Fig. 4, it is observed that when the Rayleigh number is small, isotherm surfaces are almost parallel for the smaller domain size inside the air filled region and more cluster at the larger domain inside the water filled region. However, at higher Ra_a, the isotherm profiles tend to be more flat in the water filled domain. In the air filled domain, a higher Ra_a indicates non-uniform distribution of temperature resulting better heat transfer. Similarly, from Fig. 5, it is found that heatlines are quite parallel at the air filled domain for low Rayleigh number indicating less circulation. At higher Rayleigh number, with the increase of domain size, circulation inside the domain becomes intense resulting chaotic mixing of heatline patterns. This is because the buoyancy force generated for each convective domain plays a significant role here. The water filled domain shows less circulation at lower Ra_a compared to the air filled domain. Moreover, it can be seen that the heatline plots are more concentrated at the centre of the water filled domain at lower Ra_a because water is more dense than air.

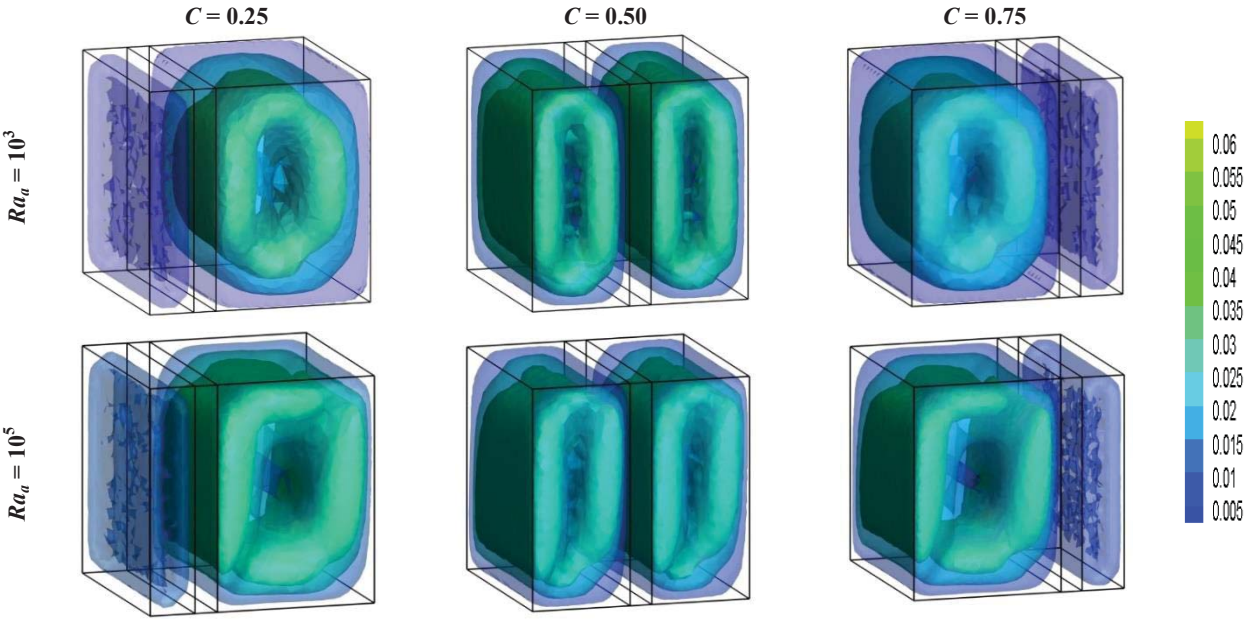

FIGURE 3. Isosurface contour maps of velocity inside the cavity for different partition positions and Rayleigh numbers.

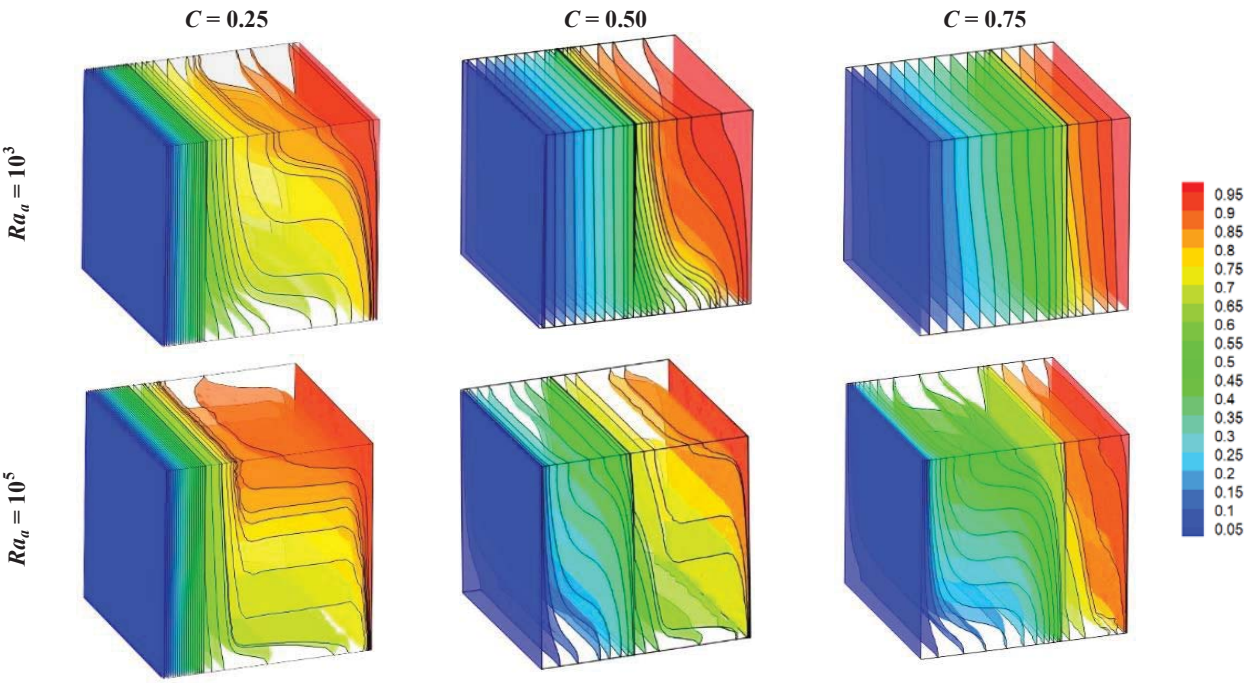

FIGURE 4. Isosurfaces of temperature profile inside the cavity for different partition positions and Rayleigh numbers.

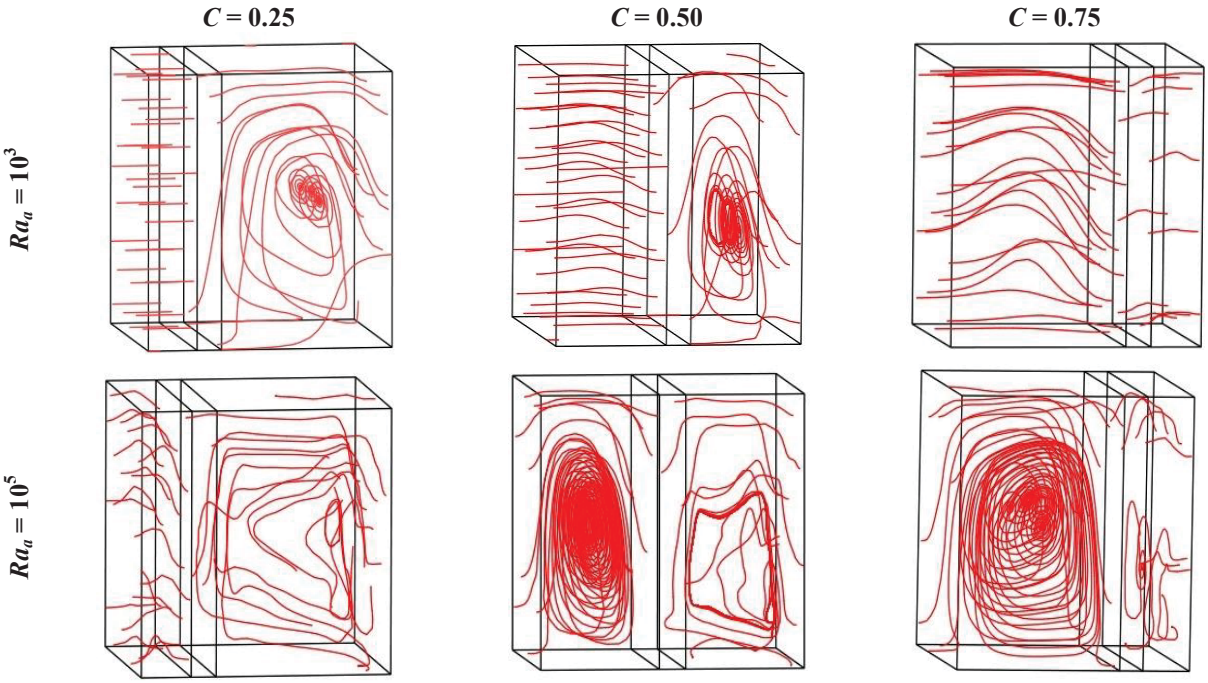

FIGURE 5. Heatlines inside the cavity for different partition positions and Rayleigh number.

Comparison of Thermal Performance between 2D and 3D model

A comparison of average Nusselt number of both hot and cold walls between 2D model of Kushwaha *et al.* [10] and 3D model of the present study is presented in Fig. 6. It is observed that as Ra_a increases, *Nu* gradually increases. The pattern of this change of *Nu* is similar for both convective domains. Besides, the effect of buoyancy force as

mentioned earlier plays an important role on the increment of heat transfer rate. *Nu* for the air filled domain is always greater than that for the water filled domain. Since greater circulation is observed within the air filled domain due to higher buoyancy force. By comparing both 2D and 3D models, it is found that the change of *Nu* of the cold wall with respect to Ra_a is similar for both models. This is also applicable for all three positions of the partition (i.e., C = 0.25, 0.50 and 0.75). For the hot wall, at the partition position C = 0.25, *Nu* computed in 3D model first increases slightly up to $Ra_a = 10^4$, then falls slightly to $Ra_a = 10^5$ and sharply increases further. Whereas in 2D model, *Nu* remains nearly the same up to $Ra_a = 10^5$ and then, suddenly rises afterwards. However, this discrepancy between both models is nearly negligible. For the other partition positions, *Nu* of the hot wall remains close to each other for both models.

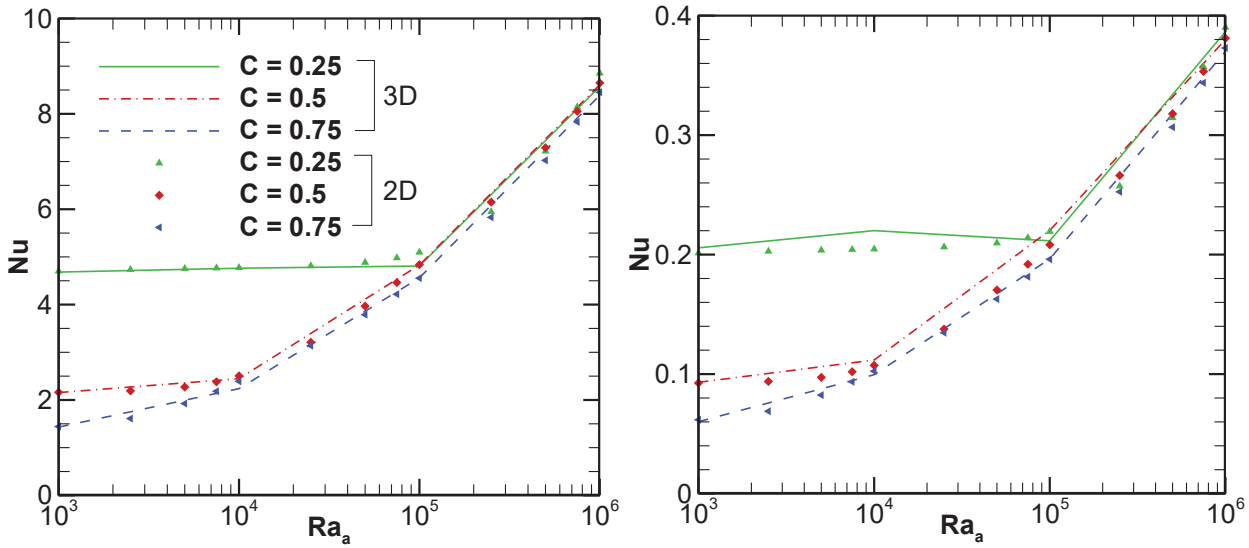

FIGURE 6. Comparison of average Nusselt number of (a) the cold wall and (b) the hot wall between 2D and 3D models as a function of Rayleigh number and the partition position.

CONCLUSION

In this study, conjugate natural convection in a three-dimensional partitioned cubic cavity filled with air and water has been investigated. The solid brick wall partition separates the cavity into air and water regions. Numerical simulation is carried out with the change of partition position over a range of Rayleigh number ($10^3 \leq Ra_a \leq 10^5$). At first, 3D visualization of flow and thermal fields are presented in terms of isosurface plots of velocity and temperature and contour plots of heat function. It is observed that better mixing and heat transfer occur inside the air domain at higher Rayleigh number. In order to compare thermal performance of the cavity, the average Nusselt number as a function of Rayleigh number is plotted for different partition position based on the results of both 2D and 3D analysis. There is no significant difference of thermal performance between 2D and 3D models. However, with the change of partition position as well as Rayleigh number, average Nusselt numbers of both hot and cold walls change significantly. Beside, the average Nusselt number follows the exact similar pattern for both hot and cold walls. It is also observed that heat transfer increases with the increment of Rayleigh number. Comparative analysis reveals that average Nusselt number decreases with the increment of partition position from the cold wall. At fixed partition position, the air domain shows higher heat transfer rate with Ra_a, since fluid circulation drastically increases in the air domain.

ACKNOWLEDGEMENT

The authors thankfully acknowledge the support provided by department of mechanical engineering of Bangladesh University of Engineering and Technology (BUET) during this research work.

REFERENCES

1. R. Anderson and A. Bejan, Int. J. Heat Mass Tran. **24**, 1611–1620 (1981).
2. D. M. Kim and R. Viskanta, J. Heat Tran. **107**, 139–146 (1985).
3. D. A. Kaminski and C. Prakash, Int. J. Heat Mass Tran. **29**, 1979–1988 (1986).
4. T. Nishimura, M. Shiraishi, F. Nagasawa and Y. Kawamura, Int. J. Heat Mass Tran. **31**, 1679–1686 (1988).
5. A. Kangni, R. B. Yedder and E. Bilgen, Int. J. Heat Mass Tran. **34**, 2819–2825 (1991).
6. P. K. Ghosh, A. Sarkar and V. M. K. Sastri, Numer. Heat Tran. **21**, 231–248 (1992).
7. S. C. Saha, M. M. Molla, S. Saha and Y. T. Gu, "Natural convection of coupled thermal boundary layers adjacent to a wavy conducting partition placed in a square differential heated enclosure", in 11th International Conference on Mechanical Engineering (Dhaka, Bangladesh, 2015).
8. M. Khatamifar, W. Lin, S. W. Armfield, D. Holmes and M. P. Kirkpatrick, Int. Commun. Heat Mass Tran. **81**, 92–103 (2017).
9. H. F. Öztop, Y. Varol and A. Koca, Int. J. Heat Mass Tran. **52**, 5909–5921 (2009).
10. B. Kushwaha, S. Barua, S. Saha, S. C. Saha, "Conjugate natural convection in a differentially heated square cavity divided by a conducting solid partition into two fluid zones," Int. J. Heat Fluid Flow (unpublished).
11. F. Selimefendigil and H. F. Öztop, Int. J. Heat Mass Tran. **139**, 1000–1017 (2019).
12. S. Kimura and A. Bejan, ASME J. Heat Tran. **105**, 916919 (1983).
13. K. Hooman and H. Gurgenci, ASME J. Heat Tran. **130**, 012501 (2008).
14. A. K. Hussein and S. H. Hussain, Alex. Eng. J. **55**, 169–186, (2016).
15. Y. A. Cengel, A. J. Ghajar, *Heat and Mass Transfer: Fundamentals and Applications* (McGrawHill Education, India, 2016), pp. 918, 924.